Pol κ is localized in the nucleus, most of the molecules are out of replication foci even after DNA damage, suggesting a role other than DNA synthesis [Ogi et al., 2005]. Currently, there is no evidence that Pol κ interacts with any of the proteins involved in repair of oxidized dNTPs. However, this possibility may need further investigation.

Group 3 includes MMS and EMS (Table II and Fig. 2C). For these chemicals, CD cells exhibited higher sensitivity than KO and WT cells. The results suggest that the expressed inactive Pol κ is negatively dominant over other proteins involved in repair of DNA damage induced by these chemicals. For example, base damages by alkylating agents such as MMS and EMS are predominantly repaired by BER where DNA glycosylases remove the damaged bases and Pol β fills the gap in DNA [Almeida and Sobol, 2007]. Thus, we speculate that the inactive Pol κ might compete with repair proteins at the damaged sites and interfere with their functions. Because MMC also exhibited slightly higher sensitivity in CD cells compared to KO cells, the inactive Pol κ may have some dominant negative effects on the repair of lesions induced by these chemicals. The finding that KO and WT cells exhibited similar cytotoxic sensitivities to MMS is consistent with the reports that *Polk*$^{-/-}$ chicken DT40 cells do not display notable increased sensitivity to MMS [Okada et al., 2002]. However, *Polk*$^{-/-}$ mouse embryonic stem (ES) cells and MEF cells are moderately sensitive to MMS [Takenaka et al., 2006]. Therefore, Pols involved in the protection of cells from MMS may vary in different species.

Group 4 includes UV, etoposide, potassium bromated, and hydroxyurea (Table II and Fig. 2D). For UV and these chemicals (except for hydroxyurea, see below), all three types of cells displayed very similar sensitivity, suggesting that Pol κ does not play a substantial role in protecting cells from cytotoxic effects induced by UV and these chemicals in vivo. However, some of the results are not consistent with previous results in vivo and somewhat unexpected. For example, our results are inconsistent with the reports that *Polk*$^{-/-}$ mouse ES cells and chicken DT40 cells are sensitive to the killing effects of UV irradiation [Ogi et al., 2002; Okada et al., 2002]. The result that mouse cells exhibit UV sensitivity, even though Pol κ itself does not bypass across UV-induced lesions in vitro, are explained by the reduced nucleotide excision repair (NER) activity in *Polk*$^{-/-}$ cells [Ogi and Lehmann, 2006]. Pol κ is supposed to carry out repair DNA synthesis together with replicative Pols at the late step of NER [Ogi et al., 2010]. The reason for the apparent discrepancy between our results and the previous results is uncertain, but the concentrations of dNTPs in the cells may be involved. It has been suggested that Pol κ may play a more substantial role in the repair synthesis in NER when the concentrations of dNTPs are tightened [Ogi and Lehmann, 2006]. By analogy, we speculate that Nalm-6-MSH+ cells might have higher concentrations of dNTPs compared to mouse ES cells or chicken DT40 cells, which might be the reason why Pol κ did not exhibit any detectable roles in protection of cells against UV irradiation in Nalm-6-MSH+ cells. In general, proliferative cells such as cancer cells have higher dNTPs than normal cells for rapid proliferation. Unexpected results with chemicals in Group 4 were that KO cells displayed increased resistance to the killing effects of hydroxyurea compared to WT and CD cells. In this regard, hydroxyurea may be an exception in Group 4. The results suggest that Pol κ may be detrimental for survival of cells in the presence of hydroxyurea regardless of the Pol activity. As described above, most of Pol κ molecules are out of the replication foci in the nucleus, but they seem to enter the foci when the dNTP concentrations are lowered by the addition of hydroxyurea [Ogi et al., 2005]. We speculate that the excess presence of Pol κ in the replication foci, regardless of the Pol activity, might be harmful to the chromosome replication, which reduces the cell survival. Over commitment of Pol κ in chromosome replication may be detrimental for cell survival and genome integrity [Bavoux et al., 2005; Jones et al., 2012]. It is known that DinB, the bacterial counterpart, induces cell toxicity when overexpressed [Foti et al., 2012].

In summary, we established human cell lines where expression of Pol κ is shut down (KO cells) or the inactive Pol κ is expressed (CD cells), and compared the cytotoxic sensitivity with WT cells to 11 genotoxins. The results suggest that Pol κ protects human cells not only as a specialized Pol but also as a non-catalytic protein. As a catalytic protein, Pol κ appears to bypass N^2-guanyl adducts of BPDE and DNA crosslinks induced by MMC, which enhances the survival of cells exposed to these chemicals. In addition, Pol κ might play a role in HR, thereby protecting cells from bleomycin, which induces DSBs in DNA. As a non-catalytic protein, Pol κ may interact with other protein(s) and protect cells from oxidative damage in DNA induced by hydrogen peroxide and menadione. Possible candidates for interaction are other specialized Pol such as Pol ι involved in BER or repair proteins involved in sanitization of oxidized dNTPs. The results also reveal that the inactive Pol κ may have dominant negative effects on repair of alkylation damage in DNA. Overall, the results emphasize the importance of cellular experiments to examine the in vitro findings to investigate the significance of Pol κ in protection of human cells from various genotoxic stresses.

AUTHOR CONTRIBUTIONS

Dr. Takehiko Nohmi has designed the basic framework of this study. Drs. Tetsuya Suzuki and Peter Grúz also

contributed to the study design. Mr. Yuki Kanemaru, Drs. Naoko Niimi and Tetsuya Suzuki conducted the experiments. Drs. Noritaka Adachi, Kyomu Matsumoto and Masamitsu Honma advised the people involved in the experiments. Mr. Yuki Kanemaru and Dr. Takehiko Nohmi drafted the manuscript and all authors approved the final manuscript.

REFERENCES

Adachi N, Iiizumi S, So S, Koyama H. 2004. Genetic evidence for involvement of two distinct nonhomologous end-joining pathways in repair of topoisomerase II-mediated DNA damage. Biochem Biophys Res Commun 318:856–861.

Adachi N, So S, Iiizumi S, Nomura Y, Murai K, Yamakawa C, Miyagawa K, Koyama H. 2006. The human pre-B cell line Nalm-6 is highly proficient in gene targeting by homologous recombination. DNA Cell Biol 25:19–24.

Almeida KH, Sobol RW. 2007. A unified view of base excision repair: Lesion-dependent protein complexes regulated by post-translational modification. DNA Repair (Amst) 6:695–711.

Avkin S, Goldsmith M, Velasco-Miguel S, Geacintov N, Friedberg EC, Livneh Z. 2004. Quantitative analysis of translesion DNA synthesis across a benzo[*a*]pyrene-guanine adduct in mammalian cells: The role of DNA polymerase kappa. J Biol Chem 279: 53298–53305.

Baptiste BA, Eckert KA. 2012. DNA polymerase kappa microsatellite synthesis: Two distinct mechanisms of slippage-mediated errors. Environ Mol Mutagen 53:787–796.

Bavoux C, Leopoldino AM, Bergoglio V, Wang J, Ogi T, Bieth A, Judde JG, Pena SD, Poupon MF, Helleday T, et al. 2005. Up-regulation of the error-prone DNA polymerase κ promotes pleiotropic genetic alterations and tumorigenesis. Cancer Res 65:325–330.

Bebenek K, Tissier A, Frank EG, McDonald JP, Prasad R, Wilson SH, Woodgate R, Kunkel TA. 2001. 5'-Deoxyribose phosphate lyase activity of human DNA polymerase iota *in vitro*. Science 291: 2156–2159.

Betous R, Pillaire MJ, Pierini L, van der Laan S, Recolin B, Ohl-Seguy E, Guo C, Niimi N, Gruz P, Nohmi T, et al. 2013. DNA polymerase kappa-dependent DNA synthesis at stalled replication forks is important for CHK1 activation. EMBO J 32:2172–2185.

Chen J, Stubbe J. 2005. Bleomycins: Towards better therapeutics. Nat Rev Cancer 5:102–112.

Choi JY, Angel KC, Guengerich FP. 2006. Translesion synthesis across bulky N^2-alkyl guanine DNA adducts by human DNA polymerase k. J Biol Chem 281:21062–21072.

Clements J. 2000. The mouse lymphoma assay. Mutat Res 455:97–110.

Fischhaber PL, Gerlach VL, Feaver WJ, Hatahet Z, Wallace SS, Friedberg EC. 2002. Human DNA polymerase k bypasses and extends beyond thymine glycols during translesion synthesis *in vitro*, preferentially incorporating correct nucleotides. J Biol Chem 277:37604–37611.

Foti JJ, Devadoss B, Winkler JA, Collins JJ, Walker GC. 2012. Oxidation of the guanine nucleotide pool underlies cell death by bactericidal antibiotics. Science 336:315–319.

Friedberg EC, Wagner R, Radman M. 2002. Specialized DNA polymerases, cellular survival, and the genesis of mutations. Science 296:1627–1630.

Friedberg EC, Lehmann AR, Fuchs RP. 2005. Trading places: How do DNA polymerases switch during translesion DNA synthesis? Mol Cell 18:499–505.

Fukuda H, Takamura-Enya T, Masuda Y, Nohmi T, Seki C, Kamiya K, Sugimura T, Masutani C, Hanaoka F, Nakagama H. 2009. Translesional DNA synthesis through a C8-guanyl adduct of 2-amino-1-methyl-6-phenylimidazo[4,5-*b*]pyridine (PhIP) in vitro: Rev1 inserts dc opposite the lesion and DNA polymerase kappa potentially catalyzes extension reaction from the 3'-dC terminus. J Biol Chem 284:25585–25592.

Gerlach VL, Aravind L, Gotway G, Schultz RA, Koonin EV, Friedberg EC. 1999. Human and mouse homologs of *Escherichia coli* DinB (DNA polymerase IV), members of the UmuC/DinB superfamily. Proc Natl Acad Sci USA 96:11922–11927.

Gruz P, Pisani FM, Shimizu M, Yamada M, Hayashi I, Morikawa K, Nohmi T. 2001. Synthetic activity of Sso DNA polymerase Y1, an archaeal DinB-like DNA polymerase, is stimulated by processivity factors proliferating cell nuclear antigen and replication factor C. J Biol Chem 276:47394–47401.

Haracska L, Prakash L, Prakash S. 2002. Role of human DNA polymerase kappa as an extender in translesion synthesis. Proc Natl Acad Sci USA 99:16000–16005.

Huang X, Kolbanovskiy A, Wu X, Zhang Y, Wang Z, Zhuang P, Amin S, Geacintov NE. 2003. Effects of base sequence context on translesion synthesis past a bulky (+)-*trans-anti*-B[*a*]P-*N2*-dG lesion catalyzed by the Y-family polymerase pol κ. Biochemistry 42:2456–2466. .

Iiizumi S, Nomura Y, So S, Uegaki K, Aoki K, Shibahara K, Adachi N, Koyama H. 2006. Simple one-week method to construct gene-targeting vectors: Application to production of human knockout cell lines. Biotechniques 41:311–316.

Jaloszynski P, Ohashi E, Ohmori H, Nishimura S. 2005. Error-prone and inefficient replication across 8-hydroxyguanine (8-oxoguanine) in human and mouse ras gene fragments by DNA polymerase kappa. Genes Cells 10:543–550.

Johnson RE, Kondratick CM, Prakash S, Prakash L. 1999. hRAD30 mutations in the variant form of xeroderma pigmentosum. Science 285:263–265.

Jones MJ, Colnaghi L, Huang TT. 2012. Dysregulation of DNA polymerase kappa recruitment to replication forks results in genomic instability. EMBO J 31:908–918.

Kamiya H, Kurokawa M. 2012. Mutagenic bypass of 8-oxo-7,8-dihydroguanine (8-hydroxyguanine) by DNA polymerase kappa in human cells. Chem Res Toxicol 25:1771–1776.

Kanagaraj R, Parasuraman P, Mihaljevic B, van LB, Burdova K, Konig C, Furrer A, Bohr VA, Hubscher U, Janscak P. 2012. Involvement of Werner syndrome protein in MUTYH-mediated repair of oxidative DNA damage. Nucleic Acids Res 40:8449–8459.

Kawanishi S, Murata M. 2006. Mechanism of DNA damage induced by bromate differs from general types of oxidative stress. Toxicology 221:172–178.

Lange SS, Takata K, Wood RD. 2011. DNA polymerases and cancer. Nat Rev Cancer 11:96–110.

Lone S, Townson SA, Uljon SN, Johnson RE, Brahma A, Nair DT, Prakash S, Prakash L, Aggarwal AK. 2007. Human DNA polymerase k encircles DNA: Implications for mismatch extension and lesion bypass. Mol Cell 25:601–614.

Lv L, Wang F, Ma X, Yang Y, Wang Z, Liu H, Li X, Liu Z, Zhang T, Huang M, et al. 2013. Mismatch repair protein MSH2 regulates translesion DNA synthesis following exposure of cells to UV radiation. Nucleic Acids Res 41:10312–10322.

Maddukuri L, Ketkar A, Eddy S, Zafar MK, Eoff RL. The Werner syndrome protein limits the error-prone 8-oxo-dG lesion bypass activity of human DNA polymerase kappa. Nucleic Acids Res (in press).

Masutani C, Kusumoto R, Yamada A, Dohmae N, Yokoi M, Yuasa M, Araki M, Iwai S, Takio K, Hanaoka F. 1999. The *XPV* (xeroderma pigmentosum variant) gene encodes human DNA polymerase eta. Nature 399:700–704.

Masutani C, Kusumoto R, Iwai S, Hanaoka F. 2000. Mechanisms of accurate translesion synthesis by human DNA polymerase eta. EMBO J 19:3100–3109.

McCulloch SD, Kunkel TA. 2008. The fidelity of DNA synthesis by eukaryotic replicative and translesion synthesis polymerases. Cell Res 18:148–161.

Minko IG, Harbut MB, Kozekov ID, Kozekova A, Jakobs PM, Olson SB, Moses RE, Harris TM, Rizzo CJ, Lloyd RS. 2008. Role for DNA polymerase kappa in the processing of N^2-N^2-guanine interstrand cross-links. J Biol Chem 283:17075–17082.

Niimi N, Sassa A, Katafuchi A, Gruz P, Fujimoto H, Bonala RR, Johnson F, Ohta T, Nohmi T. 2009. The steric gate amino acid tyrosine 112 is required for efficient mismatched-primer extension by human DNA polymerase kappa. Biochemistry 48:4239–4246.

Nohmi T. 2006. Environmental stress and lesion-bypass DNA polymerases. Annu Rev Microbiol 60:231–253.

Ogi T, Lehmann AR. 2006. The Y-family DNA polymerase kappa (pol kappa) functions in mammalian nucleotide-excision repair. Nat Cell Biol 8:640–642.

Ogi T, Kato T Jr, Kato T, Ohmori H. 1999. Mutation enhancement by DINB1, a mammalian homologue of the *Escherichia coli* mutagenesis protein *dinB*. Genes Cells 4:607–618.

Ogi T, Shinkai Y, Tanaka K, Ohmori H. 2002. Polk protects mammalian cells against the lethal and mutagenic effects of benzo[*a*]pyrene. Proc Natl Acad Sci USA 99:15548–15553.

Ogi T, Kannouche P, Lehmann AR. 2005. Localisation of human Y-family DNA polymerase kappa: Relationship to PCNA foci. J Cell Sci 118:129–136.

Ogi T, Limsirichaikul S, Overmeer RM, Volker M, Takenaka K, Cloney R, Nakazawa Y, Niimi A, Miki Y, Jaspers NG, et al. 2010. Three DNA polymerases, recruited by different mechanisms, carry out NER repair synthesis in human cells. Mol Cell 37:714–727.

Ohashi E, Murakumo Y, Kanjo N, Akagi J, Masutani C, Hanaoka F, Ohmori H. 2004. Interaction of hREV1 with three human Y-family DNA polymerases. Genes Cells 9:523–531.

Ohashi E, Hanafusa T, Kamei K, Song I, Tomida J, Hashimoto H, Vaziri C, Ohmori H. 2009. Identification of a novel REV1-interacting motif necessary for DNA polymerase kappa function. Genes Cells 14:101–111.

Ohmori H, Friedberg EC, Fuchs RP, Goodman MF, Hanaoka F, Hinkle D, Kunkel TA, Lawrence CW, Livneh Z, Nohmi T, et al. 2001. The Y-family of DNA polymerases. Mol Cell 8:7–8.

Okada T, Sonoda E, Yamashita YM, Koyoshi S, Tateishi S, Yamaizumi M, Takata M, Ogawa O, Takeda S. 2002. Involvement of vertebrate polkappa in Rad18-independent postreplication repair of UV damage. J Biol Chem 277:48690–48695.

Petta TB, Nakajima S, Zlatanou A, Despras E, Couve-Privat S, Ishchenko A, Sarasin A, Yasui A, Kannouche P. 2008. Human DNA polymerase iota protects cells against oxidative stress. EMBO J 27:2883–2895.

Povirk LF. 1996. DNA damage and mutagenesis by radiomimetic DNA-cleaving agents: Bleomycin, neocarzinostatin and other enediynes. Mutat Res 355:71–89.

Prakash S, Johnson RE, Prakash L. 2005. Eukaryotic translesion synthesis DNA polymerases: Specificity of structure and function. Annu Rev Biochem 74:317–353.

Rajao MA, Passos-Silva DG, DaRocha WD, Franco GR, Macedo AM, Pena SD, Teixeira SM, Machado CR. 2009. DNA polymerase kappa from *Trypanosoma cruzi* localizes to the mitochondria, bypasses 8-oxoguanine lesions and performs DNA synthesis in a recombination intermediate. Mol Microbiol 71:185–197.

Sale JE, Lehmann AR, Woodgate R. 2012. Y-family DNA polymerases and their role in tolerance of cellular DNA damage. Nat Rev Mol Cell Biol 13:141–152.

Sassa A, Niimi N, Fujimoto H, Katafuchi A, Gruz P, Yasui M, Gupta RC, Johnson F, Ohta T, Nohmi T. 2011. Phenylalanine 171 is a molecular brake for translesion synthesis across benzo[*a*]pyrene-guanine adducts by human DNA polymerase kappa. Mutat Res 718:10–17.

Sassa A, Suzuki T, Kanemaru Y, Niimi N, Fujimoto H, Katafuchi A, Gruz P, Yasui M, Gupta RC, Johnson F, et al. 2014. In vivo evidence that phenylalanine 171 acts as a molecular brake for translesion DNA synthesis across benzo[*a*]pyrene DNA adducts by human DNA polymerase kappa. DNA Repair (Amst) 15:21–28.

Schmitt MW, Matsumoto Y, Loeb LA. 2009. High fidelity and lesion bypass capability of human DNA polymerase delta. Biochimie 91:1163–1172.

Sekiguchi M, Tsuzuki T. 2002. Oxidative nucleotide damage: Consequences and prevention. Oncogene 21:8895–8904.

Suzuki N, Ohashi E, Kolbanovskiy A, Geacintov NE, Grollman AP, Ohmori H, Shibutani S. 2002. Translesion synthesis by human DNA polymerase k on a DNA template containing a single stereoisomer of dG-(+)- or dG-(−)-*anti-N2*-BPDE (7,8-dihydroxy-*anti*−9,10-epoxy-7,8,9,10-tetrahydrobenzo[*a*]pyrene). Biochemistry 41:6100–6106.

Suzuki T, Ukai A, Honma M, Adachi N, Nohmi T. 2013. Restoration of mismatch repair functions in human cell line Nalm-6, which has high efficiency for gene targeting. PLoS One 8:e61189.

Takeiri A, Wada NA, Motoyama S, Matsuzaki K, Tateishi H, Matsumoto K, Niimi N, Sassa A, Gruz P, Masumura K, et al. 2014. *In vivo* evidence that DNA polymerase kappa is responsible for error-free bypass across DNA cross-links induced by mitomycin C. DNA Repair (Amst) 24:113–121.

Takenaka K, Ogi T, Okada T, Sonoda E, Guo C, Friedberg EC, Takeda S. 2006. Involvement of vertebrate Polk in translesion DNA synthesis across DNA monoalkylation damage. J Biol Chem 281: 2000–2004.

Ulrich HD, Takahashi T. 2013. Readers of PCNA modifications. Chromosoma 122:259–274.

Vermeulen C, Bertocci B, Begg AC, Vens C. 2007. Ionizing radiation sensitivity of DNA polymerase lambda-deficient cells. Radiat Res 168:683–688.

Wagner J, Gruz P, Kim SR, Yamada M, Matsui K, Fuchs RP, Nohmi T. 1999. The *dinB* gene encodes a novel *E. coli* DNA polymerase, DNA pol IV, involved in mutagenesis. Mol Cell 4: 281–286.

Wojtaszek J, Lee CJ, D'Souza S, Minesinger B, Kim H, D'Andrea AD, Walker GC, Zhou P. 2012a. Structural basis of Rev1-mediated assembly of a quaternary vertebrate translesion polymerase complex consisting of Rev1, heterodimeric polymerase (Pol) zeta, and Pol kappa. J Biol Chem 287:33836–33846.

Wojtaszek J, Liu J, D'Souza S, Wang S, Xue Y, Walker GC, Zhou P. 2012b. Multifaceted recognition of vertebrate Rev1 by translesion polymerases zeta and kappa. J Biol Chem 287:26400–26408.

Yoon JH, Bhatia G, Prakash S, Prakash L. 2010. Error-free replicative bypass of thymine glycol by the combined action of DNA polymerases kappa and zeta in human cells. Proc Natl Acad Sci USA 107:14116–14121.

Yoon JH, Acharya N, Park J, Basu D, Prakash S, Prakash L. 2014. Identification of two functional PCNA-binding domains in human DNA polymerase kappa. Genes Cells 19:594–601.

Yoshimura D, Sakumi K, Ohno M, Sakai Y, Furuichi M, Iwai S, Nakabeppu Y. 2003. An oxidized purine nucleoside triphosphatase, MTH1, suppresses cell death caused by oxidative stress. J Biol Chem 278:37965–37973.

Yuan B, You C, Andersen N, Jiang Y, Moriya M, O'Connor TR, Wang Y. 2011. The roles of DNA polymerases kappa and iota in the error-free bypass of N^2-carboxyalkyl-2′-deoxyguanosine lesions in mammalian cells. J Biol Chem 286:17503–17511.

Zhang Y, Yuan F, Wu X, Wang M, Rechkoblit O, Taylor JS, Geacintov NE, Wang Z. 2000. Error-free and error-prone lesion bypass by human DNA polymerase k *in vitro*. Nucleic Acids Res 28:4138–4146.

Zhang X, Lv L, Chen Q, Yuan F, Zhang T, Yang Y, Zhang H, Wang Y, Jia Y, Qian L, et al. 2013. Mouse DNA polymerase kappa has a functional role in the repair of DNA strand breaks. DNA Repair (Amst) 12:377–388.

Zlatanou A, Despras E, Braz-Petta T, Boubakour-Azzouz I, Pouvelle C, Stewart GS, Nakajima S, Yasui A, Ishchenko AA, Kannouche PL. 2011. The hMsh2-hMsh6 complex acts in concert with monoubiquitinated PCNA and Pol eta in response to oxidative DNA damage in human cells. Mol Cell 43:649–662.

Accepted by—
O. Schärer

Published online 18 June 2015

Nucleic Acids Research, 2015, Vol. 43, No. 13 ***6359–6372***
doi: 10.1093/nar/gkv621

Smarcal1 promotes double-strand-break repair by nonhomologous end-joining

Islam Shamima Keka[1], Mohiuddin[1], Yuko Maede[1], Md Maminur Rahman[1], Tetsushi Sakuma[2], Masamitsu Honma[3], Takashi Yamamoto[2], Shunichi Takeda[1] and Hiroyuki Sasanuma[1,*]

[1]Department of Radiation Genetics, Kyoto University, Graduate School of Medicine, Yoshida Konoe, Sakyo-ku, Kyoto 606-8501, Japan, [2]Department of Mathematical and Life Sciences, Graduate School of Science, Hiroshima University, Higashi-Hiroshima 739-8526, Japan and [3]Division of Genetics and Mutagenesis, National Institute of Health Sciences, 1-18-1 Kamiyoga, Setagaya-ku, Tokyo 158-8501, Japan

Received February 27, 2015; Revised May 29, 2015; Accepted June 03, 2015

ABSTRACT

Smarcal1 is a SWI/SNF-family protein with an ATPase domain involved in DNA-annealing activities and a binding site for the RPA single-strand-DNA-binding protein. Although the role played by Smarcal1 in the maintenance of replication forks has been established, it remains unknown whether Smarcal1 contributes to genomic DNA maintenance outside of the S phase. We disrupted the *SMARCAL1* gene in both the chicken DT40 and the human TK6 B cell lines. The resulting *SMARCAL1*$^{-/-}$ clones exhibited sensitivity to chemotherapeutic topoisomerase 2 inhibitors, just as nonhomologous end-joining (NHEJ) null-deficient cells do. *SMARCAL1*$^{-/-}$ cells also exhibited an increase in radiosensitivity in the G_1 phase. Moreover, the loss of Smarcal1 in NHEJ null-deficient cells does not further increase their radiosensitivity. These results demonstrate that Smarcal1 is required for efficient NHEJ-mediated DSB repair. Both inactivation of the ATPase domain and deletion of the RPA-binding site cause the same phenotype as does null-mutation of Smarcal1, suggesting that Smarcal1 enhances NHEJ, presumably by interacting with RPA at unwound single-strand sequences and then facilitating annealing at DSB ends. *SMARCAL1*$^{-/-}$cells showed a poor accumulation of Ku70/DNA-PKcs and XRCC4 at DNA-damage sites. We propose that Smarcal1 maintains the duplex status of DSBs to ensure proper recruitment of NHEJ factors to DSB sites.

INTRODUCTION

Smarcal1 (a SWI/SNF-related, matrix associated, actin-dependent regulator of chromatin a-like 1) is a SWI/SNF family protein that carries an ATPase domain and the binding site for replication protein A (RPA), the single-strand-DNA-binding protein (1,2). Smarcal1 is an ATP-driven annealing helicase that catalyzes the formation of double-strand DNA from complementary single-strand DNA strands associated with RPA. Thus, Smarcal1 could counteract unwinding by DNA helicases at DSB sites. The annealing activity is stimulated by substrate DNA containing both single-strand and double-strand regions, such as a chicken foot structure (3). Mutations in the *SMARCAL1* gene cause a rare autosomal recessive disease, Schimke immuno-osseous dysplasia (SIOD), which is characterized by short stature, kidney disease and a severely compromised immune system (4–7). Phenotypic analysis of Smarcal1-depleted cells suggests that Smarcal1 stabilizes replication forks when cells are exposed to aphidicolin, hydroxyurea and camptothecin (a topoisomerase 1 poison) (1,2,8–10).

The two major double-strand-break (DSB) repair pathways, homologous recombination (HR) and nonhomologous end-joining (NHEJ) (11–13) significantly contribute to cellular tolerance to anti-malignant therapies. First, both pathways contribute to cellular tolerance to radiotherapy, HR in the S to G_2 phases and NHEJ throughout the cell cycle. Second, HR plays the dominant role in repairing DSBs generated during DNA replication by chemotherapeutic agents such as camptothecin and poly[ADP ribose]polymerase inhibitor (olaparib). These chemotherapeutic agents cause the accumulation of single-strand breaks, which are converted by DNA replication to DSBs called one-end breaks. These DSBs are repaired by HR but not by NHEJ (14–16). Third, NHEJ plays the dominant role in repairing DSBs caused by chemotherapeutic topoisomerase 2 inhibitors such as ICRF193 and etoposide (15,17). Measuring the sensitivity of gene-disrupted cells to various anti-malignant therapies allows us to define the role of the gene in HR, NHEJ or both. In addition to the above, the capability of canonical NHEJ is evaluated

*To whom correspondence should be addressed. Tel: +81 75 753 4410; Fax: +81 75 753 4419; Email: hiroysasa@rg.med.kyoto-u.ac.jp

by examining the V(D)J recombination of Immunoglobulin (Ig) V genes, which requires a collaboration between NHEJ and V(D)J recombinase encoded by the recombination-activating-genes 1 and 2 (Rag1/Rag2) (18–20).

Canonical NHEJ is initiated by associating a Ku70/Ku80 heterodimer with DSB sites. Ku70/Ku80 associates preferentially with duplex DNA ends, rather than with DSBs carrying single-strand tails generated by exonucleases or DNA helicases (21–24). Ku70/Ku80 forms a complex with DNA-dependent-protein-kinase catalytic subunit (DNA-PKcs), leading to the activation of DNA-PKcs at DSB sites (25–27). DNA-PKcs phosphorylates a number of substrates, including itself (28–31). Ligase4 (Lig4) completes DSB repair in collaboration with the essential co-factors, XLF and XRCC4, which form clamp-like structures along duplex DNA (32–35). If canonical NHEJ does not perform DSB repair, non-canonical end-joining such as microhomology-mediated alternative end-joining (MMEJ) repairs DSBs, though less efficiently than canonical NHEJ, causing deletion near the DSB sites (36,37).

We disrupted the *SMARCAL1* gene in the chicken DT40 and human B lymphoblastoid TK6 cell lines (38,39). The resulting *SMARCAL1*$^{-/-}$ clones exhibited sensitivity to camptothecin, suggesting that Smarcal1 plays a role in DNA replication, as indicated previously (9,10). Remarkably, Smarcal1 is also required for efficient NHEJ in human as well as in chicken cells. This conclusion is in agreement with the fact that SIOD patients exhibit reduced V(D)J recombination products in peripheral lymphocytes as well as increased chromosomal breakage (40,41). We propose that the decreased efficiency of NHEJ in V(D)J recombination as well as the compromised maintenance of replication fork progression result in severe lymphocytopenia in SIOD patients (4,40,41).

MATERIALS AND METHODS

Cell clones

All the clones used in this study are summarized in Table 1.

Cell culture

DT40 and TK6 cells were cultured in the same manner as described previously (39,42).

Generation of *SMARCAL1*$^{-/-}$ DT40 cells

SMARCAL1 gene disruption constructs were generated from genomic polymerase chain reaction (PCR) products combined with histidinol dehydrogenase (*hisD*) and puromycin-resistance (*puro*^{R}) marker genes. Genomic DNA from *wild-type* cells was amplified using the F1 and R1 primers for the 5′-arm and the F2 and R2 primers for the 3′-arm. The amplified 3′-arm PCR product was subcloned into pCR2.1-TOPO vector (Invitrogen, US). The 5′-arm PCR product harboring the *Sac*I and *Bam*HI sites at the 5′- and 3′-ends, respectively, was cloned into the *Sac*I and *Bam*HI sites of the pCR2.1-TOPO vector carrying the 3′-arm. The *Bam*HI fragment containing either the *hisD* or *puro*^{R} gene was cloned into the *Bam*HI site between the 3′-arm and the 5′-arm in the pCR2.1-TOPO vector. To generate *SMARCAL1*$^{-/-}$ cells, the *SMARCAL1* gene-disruption constructs carrying *hisD* and *puro*^{R} were linearized, using the *Not*I restriction enzyme, and sequentially transfected by electroporation (Bio-Rad, US). A 0.5 kb probe was generated by PCR of genomic DNA using primers F3 and R3 for Southern blot analysis. The genomic DNA of the candidate clones was digested with *Sma*I and *Xho*I for Southern blot analysis. The gene disruption was confirmed by RT-PCR, using primers F4 and R4. When generating *SMARCAL1*$^{+/-}$ clones from *wild-type* cells the targeting efficiency was 20% (4/20), while that of generating *SMARCAL1*$^{-/-}$ cells from *SMARCAL1*$^{+/-}$ cells was 1.4% (1/71). All primers used here are shown in Supplemental Table S1.

Generation of *SMARCAL1*$^{\Delta 30/-}$ and *KU70*$^{-/-}$/*SMARCAL1*$^{\Delta 30/-}$ DT40 cells

The intact allele of the *SMARCAL1*$^{+/-}$ cell was targeted for deleting the first 30 amino acids, which domain is responsible for RPA binding (10). To generate the *Δ30* construct, the 5′-arm was amplified from genomic DNA using the *Not*I-tagged F5 and the *Bam*HI-tagged R5, and the 3′-arm was amplified using the *Bam*HI-tagged F6, which was designed from 90 bases downstream of start codon ATG in exon1, and the *Sal*I-tagged R6. In the Zero Blunt TOPO vector (Invitrogen, US), the left and right arms were cloned at the site of *Not*I-*Bam*HI and *Bam*HI-*Sal*I, respectively. The selection-marker gene, puromycin resistance (*puro*^{R}) flanked by *loxP* sequences, was then inserted into the *Bam*HI site between the left and right arms. The resulting *Δ30-puro*^{R} construct was transfected into the *SMARCAL1*$^{+/-}$ and *KU70*$^{-/-}$/*SMARCAL1*$^{+/-}$ cells. The *puro*^{R} gene was popped out by transient expression of cre-recombinase, resulting in the generation of *SMARCAL1*$^{\Delta 30/-}$ *and KU70*$^{-/-}$/*SMARCAL1*$^{\Delta 30/-}$ DT40 cells. To confirm the gene disruption by RT-PCR, the primer set F4 and R4 was used.

Generation of human *SMARCAL1*$^{-/-}$ and *SMARCAL1*$^{-/-}$/*LIG4*$^{-/-}$ TK6 B cells

To generate a pair of TALEN expression plasmids against the *SMARCAL1* gene, we used a Golden Gate TALEN kit and a TAL effector kit (Addgene, US) (43,44). The TALEN target sites are shown in Supplementary Figure S2. The gene-targeting constructs were generated from the genomic DNA of TK6 cells by amplifying with primers *Xho*I-flanked F7 and *Nhe*I-flanked R7 for the 5′-arm and *Not*I-flanked F8 and *Hind*III-flanked R8 for the 3′-arm. The 5′-arm PCR products were cloned into the *Xho*I and *Nhe*I sites found upstream of the *puro*^{R} and *hygro*^{R} marker genes of the DT-ApA/puro and DT-ApA/hygro vectors, respectively. The 3′-arm PCR products were cloned into the *Not*I and *Hind*III sites found downstream of the *puro*^{R} and *hygro*^{R} marker genes of the DT-ApA/puro and DT-ApA/hygro vectors, respectively. 6 μg TALEN-expression plasmids and 2 μg gene-targeting vectors were transfected into 4×10^6 TK6 cells using the Neon Transfection System (Life Technologies, US) with 3X pulse at 1350 V and

Table 1. Panel of cell lines used in this study

Genotype	Parental Cell Line	Markers genes	References
SMARCAL1$^{-/-}$	DT40	*hisD*, *puro*^{R}	*
SMARCAL1$^{\Delta 30/-}$	DT40	*hisD*	*
KU70$^{-/-}$	DT40	*bsr*^{R}, *puro*^{R}	(55)
BRCA2$^{-/-}$	DT40	*hygro*^{R}, *hisD*	(46)
KU70$^{-/-}$/*SMARCAL1*$^{\Delta 30/-}$	DT40	*hisD*, *bsr*^{R}, *puro*^{R}	*
SMARCAL1$^{-/-}$	TK6-derived TSCER2 and TSCE5	*puro*^{R}, *hygro*^{R}	* T
LIG4$^{-/-/-}$	TK6-derived TSCER2 and TSCE5	*puro*^{R}, *neo*^{R}	* C
RAD54$^{-/-}$	TK6-derived TSCER2	*puro*^{R}, *neo*^{R}	* T
SMARCAL1$^{-/-}$/*LIG4*$^{-/-/-}$	TK6-derived TSCE5	*puro*^{R}, *neo*^{R}, *hygro*^{R}	* T/C
DNA-PKcs$^{-/-}$	TK6-derived TSCE5	*neo*^{R}, *hisD*	* C
SMARCAL1$^{-/-}$/*DNA-PKcs*$^{-/-}$	TK6-derived TSCE5	*neo*^{R}, *hisD*	* T/C

* = This study; T = TALEN; C = CRISPR.

with 10 ms pulse width. After electroporation, cells were released into 20 ml drug-free medium containing 10% horse serum. Forty-eight hours later, cells were seeded into 96-well plates with both hygromycin and puromycin antibiotics for two weeks. The genomic DNAs of the isolated clones resistant to both hygromycin and puromycin were digested with *Xba*I for Southern blot analysis. A 0.6 kb probe was generated by PCR of genomic DNA using primers F9 and R9. The loss of Smarcal1-protein expression was confirmed by western blot analysis (Supplementary Figure S2B). The efficiency of generating *SMARCAL1*$^{-/-}$clones from *wild-type* cells was 100% (3/3). The method for generating *LIG4*$^{-/-/-}$ and *RAD54*$^{-/-}$ TK6 cells is described in the Supplemental Materials and Methods. *SMARCAL1*$^{-/-}$/*LIG4*$^{-/-/-}$ clones were generated by disrupting the *LIG4* gene in the *SMARCAL1*$^{-/-}$ cells. Gene-targeting efficiency was 10% (2/20).

Generation of human *DNA-PKcs*$^{-/-}$ and *SMARCAL1*$^{-/-}$/*DNA-PKcs*$^{-/-}$ TK6 B cells

To disrupt the *DNA-PKcs* gene, we designed a guide RNA targeting the 32nd exon using the Zhang CRISPR tool (45) and gene-targeting constructs. The CRISPR-target site is depicted in Supplementary Figure S3E. The gene-targeting constructs were generated using SLiCE (Seamless Ligation Cloning Extract). The genomic DNA was amplified with primers F19 and R19 from the *DNA-PKcs*-gene locus and the PCR product was used as template DNA for amplifying the 5′- and 3′-arms. The 5′-arm was amplified using primers F20 and R20 and the 3′-arm was amplified using primers F21 and R21, where each primer shared 20-base pair-end homology with the insertion site of the vector. Both vectors, DT-ApA/neo and DT-ApA/his, were linearized with *Afl*II and *Apa*I. All the fragments of the vectors and inserts were purified using a qiaquick gel extraction kit (QIAGEN, Netherlands). The gene-targeting constructs were generated in a single reaction mixture containing DT-ApA/neo or DT-ApA/his vectors, 5′- and 3′-arms, and 2×SLiCE buffer (Invitrogen, US) and incubated for 30 min at room temperature. 6 μg of CRISPR and 2 μg of each gene-targeting vector were transfected into 4×10^{6} TK6 cells using the Neon Transfection System (Life Technologies, US). After electroporation, cells were released into 20 ml drug-free medium containing 10% horse serum. Forty-eight hours later, cells were seeded into 96-well plates for selection with both neomycin and histidinol antibiotics for two weeks. The gene disruption was confirmed by RT-PCR using primers F22 and R22, and by western blot analysis with anti-DNA-PKcs antibody (Supplementary Figure S3F). The targeting efficiency of generating *DNA-PKcs*$^{-/-}$ clones from *DNA-PKcs*$^{+/+}$ cells was 90% (9/10). The targeting efficiency of generating *SMARCAL1*$^{-/-}$/*DNA-PKcs*$^{-/-}$ clones from *SMARCAL1*$^{-/-}$/*DNA-PKcs*$^{+/+}$ cells was 100% (2/2).

Generation of *SMARCAL1*$^{-/-}$ cells reconstituted with *SMARCAL1*^{WT}, *SMARCAL1*^{R764Q} or *SMARCAL1*$^{\Delta 30}$ transgene

The *SMARCAL1* cDNA was bought from the Kazusa DNA research institute (Chiba, Japan). The *SMARCAL1*^{R764Q} cDNA was obtained by site-directed mutagenesis of *SMARCAL1*^{WT} (*wild-type SMARCAL1*) cDNA using primers F18 and R18. The *SMARCAL1*$^{\Delta 30}$ cDNA with the first 30 amino acids deleted was generated from *SMARCAL1*^{WT} cDNA by PCR using primers F10 and R10. The *SMARCAL1*^{WT}, *SMARCAL1*^{R764Q} and *SMARCAL1*$^{\Delta 30}$ transgenes were cloned into pMSCV-IRES-GFP retroviral expression vector (Clontech, US). The newly engineered retroviral expression vector was co-transfected into human 293T cells with a helper plasmid (pClampho, US) to produce a viral supernatant, which was collected after 24 hours and used to infect the *SMARCAL1*$^{-/-}$ cells. The efficiency of infection was assessed by quantifying the number of cells expressing GFP using flow-cytometric analysis (LSRFortessa, BD Biosciences, US). The cells expressing GFP were enriched using a cell sorter (FACSAria III, BD Biosciences, US) and seeded into 96 well plates to isolate single colonies. The expression level of the transgenes in the *SMARCAL1*$^{-/-}$ cells was measured by western blot (Figure 5D).

Colony-survival assay

To measure sensitivity, cells were treated with camptothecin (Topogen, Inc, US) and ICRF193 (Funakoshi, Japan) (17) and irradiated with ionizing radiation (^{137}Cs). Cell sensitivity to these DNA-damaging agents was evaluated by counting colony formation in methylcellulose plates as described previously (46,47).

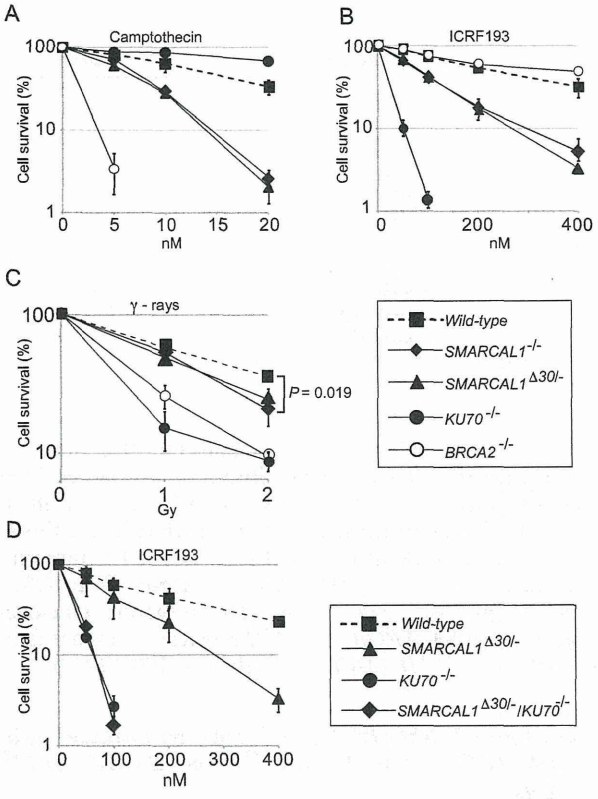

Figure 1. Smarcal1-deficient DT40 cells are sensitive to ICRF193 and camptothecin. Clonogenic-cell-survival assay following exposure of the indicated genotypes to DNA-damaging agents (**A–D**). The *x*-axis represents the dose of the indicated DNA-damaging agent on a linear scale; the *y*-axis represents the survival fraction on a logarithmic scale. Error bars show the SD of the mean for three independent assays. The *P*-value of (C) was calculated by Student's *t*-test or two-sample *t*-test for IR sensitivity at 2 Gy.

Cell-cycle synchronization

Cells were synchronized by centrifugal-counter-flow elutriation (Hitachi Koki, Japan). The cell suspension ($\sim 5 \times 10^7$ TK6 cells) was loaded at a flow rate of 15 ml/min into an elutriation chamber rotating at 2000 rpm. Cell synchrony was confirmed by FACS analysis (LSRFortessa, BD Biosciences, US).

Immunostaining and microscopic analysis

Cells were fixed with 4% paraformaldehyde (Nacalai Tesque, Japan) for 10 min at room temperature and permeabilized with 0.5% TritonX-100 (Sigma, St. Louis, US) for 20 min. To exclude S-phase cells from the count shown in Figure 3C and D, a Click-iT EdU imaging kit (Alexa594, Invitrogen, US) was used. Images were taken with a confocal microscope (TCS SP8, Leica Microsystems, Germany) and a BX-61 microscope (Olympus, Japan).

V(D)J-recombination assay

The V(D)J-recombination assay was performed as described previously (48). Briefly, 4×10^6 TK6 cells were transfected (Neon, Life Technologies, US) with 600 ng of circular pJH200 or pJH290, 5.4 μg of *RAG1*- and 6.6 μg of *RAG2*-expression vector. The extrachromosomal plasmids were recovered from cells after 48 hours using a modified Hirt extraction method (49). The mixture of 15 μl of ElectroMAX™ DH10B™ (Life Technologies, US) competent bacteria and 300 ng (range of 100–500 ng) of recovered plasmids were added to an electroporation cuvette (0.1 cm gap) and incubated on ice for 10 min. The bacteria were then electroporated at 1.8 kV, 200 Ω and 25 uF for 2 seconds using a Gene PulserII (Bio-Rad, US). Pre-warmed SOC media was added to the bacteria and the reaction was incubated at 37°C for 2 hours. The reaction was plated on LB-agar plates containing 100 μg/ml ampicillin and 10 μg/ml chloramphenicol and incubated for 16–24 hours at 37°C. The ampicillin+chloramphenicol-resistant plasmids were isolated and subjected to *Apa*LI digestion to examine the fidelity of the signal joints. Digestion of original pJH200 plasmid yields a 4.3 kb band, while that of the correct recombination products yields 3.5 kb + 0.8 kb bands due to the newly generated *Apa*LI site. Signal-joint and coding-joint sequences were analyzed using the sequencing primer R17 (50).

NHEJ assay of I-*Sce*1-induced DSBs

A TK6-derived line that is heterozygous for point mutation in exon4 of the thymidine-kinase gene ($TK^{+/-}$) was used to measure the frequency of NHEJ events as described previously (51,52). To measure the length of deletion in DSB-repair products formed in *wild-type* and $SMARCAL1^{-/-}$ cells, primers Fa and Ra were used. To measure the length of the deletion formed in the $LIG4^{-/-/-}$ cells, primers Fa and Rb were used.

Chromatin fractionation and chromatin immunoprecipitation

A Subcellular Protein Fractionation Kit from Thermo Scientific (78840) was used for chromatin fractionation. Expression plasmids for a TALEN and I-*Sce*1 were transfected into TK6 cells using the Neon Transfection System. After 20 hours, transfected cells were analyzed by western blotting and ChIP. ChIP was performed as described previously (53), with some modifications. Briefly, samples were sonicated to generate DNA fragments of <500 bp. The antibody was incubated with Dynabeads Protein G for 3 hours at 4°C. Sheared chromatin was centrifuged at 15000 rpm for 15 min at 4°C. After centrifugation, supernatants were incubated with antibody-protein G conjugates for 3 hours at 4°C. The conjugated beads were washed thoroughly with IP buffer-140, IP buffer-500, IP buffer-750, LiCl/detergent and TE. Real-time PCR was carried out as described previously (53). Sequences of primers are given in Supplemental Table S1.

Antibodies

Anti-γH2AX mouse monoclonal (1:1000, Millipore, US); anti-TP53BP1 rabbit polyclonal (1:100, Sigma, US); alexa fluor 488-conjugated anti-mouse IgG (1:1000, Molecular Probes); alexa fluor 488–conjugated anti-rabbit IgG

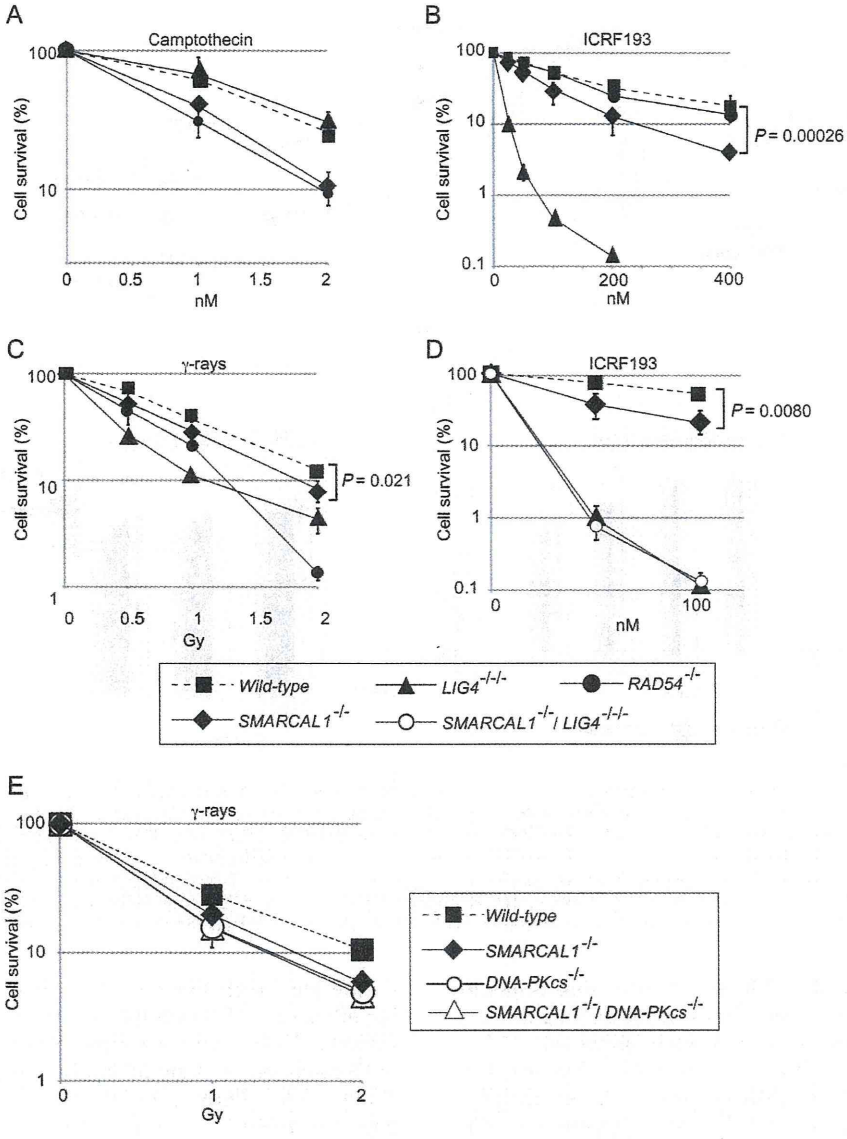

Figure 2. Sensitivity of human *SMARCAL1*$^{-/-}$, *SMARCAL1*$^{-/-}$/*LIG4*$^{-/-/-}$ and *SMARCAL1*$^{-/-}$/*DNA-PKcs*$^{-/-}$ TK6 B cells to ICRF193 and γ-rays. (**A–E**) Cellular sensitivity is shown as in Figure 1. Error bars show the SD of the mean for three independent assays. *P*-values were calculated by Student's *t*-test.

(1:1000, Molecular Probes); anti-Smarcal1 rabbit polyclonal (ab154226, abcam, UK); anti-XRCC4 goat polyclonal (C-20, Santa Cruz, US); anti-Ku70 mouse polyclonal (#GTX70270, Gene Tex, US); anti-DNA-PKcs mouse monoclonal (ab1832, abcam, UK).

RESULTS

SMARCAL1-deficient cells are sensitive to DNA-damaging agents

To analyze the role of Smarcal1 in the DSB-repair pathway, we disrupted the *SMARCAL1* gene and generated *SMARCAL1*$^{-/-}$ DT40 cells (Supplementary Figures S1A and S1C). Moreover, to selectively analyze the function of the Smarcal1-RPA interaction, we generated *SMARCAL1*$^{\Delta 30/-}$ DT40 mutant cells by deleting the N-terminal region encoding the RPA-binding site of the endogenous *SMARCAL1* gene (9) (Supplementary Figures S1D and S1E). To define the role played by Smarcal1 in various DNA-repair processes, we measured cellular responses to exogenous DNA damages. *SMARCAL1*$^{-/-}$ and *SMARCAL1*$^{\Delta 30/-}$ DT40 cells exhibited increased sensitivities to various DNA-damaging agents, including camptothecin and ICRF193 (Figures 1A and B). The sensitivity profile of the *SMARCAL1*$^{\Delta 30/-}$ cells was very similar to that of the *SMARCAL1*$^{-/-}$ cells, suggesting that the physical association of Smarcal1 with RPA is essential for its DNA-damage response (9). The elevated sen-

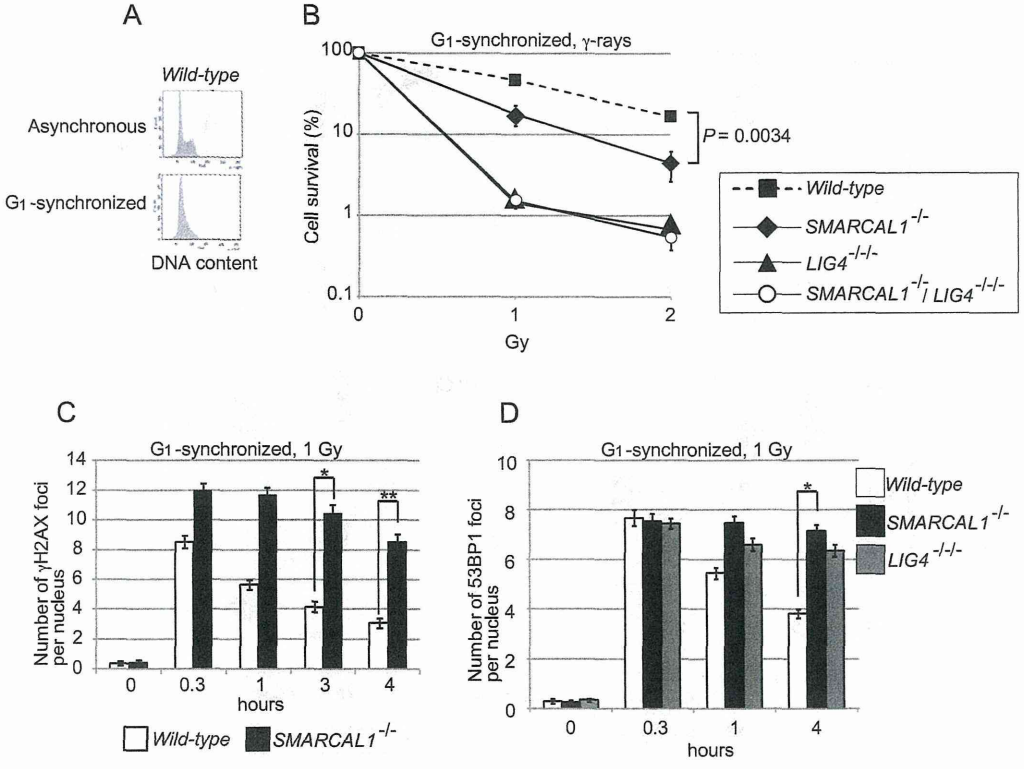

Figure 3. Repair of γ-ray induced DSBs at the G_1 phase in TK6 cells. (**A**) DNA content of G_1-synchronized TK6 cells. (**B**) Cellular sensitivity of G_1-synchronized cells to γ-rays, shown as in Figure 1. Error bars indicate the SD of the mean for three independent assays. *P*-value was calculated by Student's *t*-test. (**C**) Histogram representing the γH2AX subnuclear foci of G_1 cells after irradiation with 1 Gy γ-rays. The *x*-axis represents time after γ-irradiation (time zero); the *y*-axis represents the average number of γH2AX foci in individual cells. The nuclei of 100 morphologically intact cells were analyzed at each time point in individual experiments. The experiment was performed at least three times, with the averages presented with SD and *P*-values. Asterisks indicate statistical significance; $*P = 0.0055$ and $**P = 0.00020$. (**D**) Histogram representing the 53BP1 subnuclear foci of G_1 cells, as shown in (C). The experiment was performed at least three times, with averages presented with SD and *P*-value. Asterisks indicate statistical significance; $*p = 6.3\times10^{-5}$.

sitivity to camptothecin supports the idea that Smarcal1 helps to prevent replication forks from replication collapse at one-end breaks, as indicated previously (1,2,8–10,54). NHEJ-deficient *KU70*$^{-/-}$ cells (55), but not HR-deficient *BRCA2*$^{-/-}$cells (46), showed a hypersensitivity to ICRF193 (Figure 1B). We further analyzed the functional relationship between Smarcal1 and Ku70 by generating *KU70*$^{-/-}$/*SMARCAL1*$^{\Delta 30/-}$ double-mutant cells. The double-mutant cells showed virtually the same ICRF193 sensitivity as did the *KU70*$^{-/-}$ single mutant (Figure 1D), indicating that Smarcal1 is epistatic to Ku70.

To investigate the role of Smarcal1 in human cells, we disrupted the *SMARCAL1* gene in the human TK6 B cell line using a TALEN pair combined with gene-disruption constructs (Supplementary Figures S2A and S2B). We also generated both *LIG4*$^{-/-/-}$ (Supplementary Figures S3A and S3B) and *RAD54*$^{-/-}$ TK6 clones (Supplementary Figures S3C and S3D) as controls deficient in NHEJ and HR, respectively. In addition, we generated *DNA-PKcs*$^{-/-}$ TK6 clones (Supplementary Figures S3E and S3F). The TK6 cell line has been widely used by the governments of developed countries to detect environmental mutagens due to the very stable phenotype and karyotype of its cells (56,57). The *SMARCAL1*$^{-/-}$cells proliferated with kinetics (15 h per cell cycle) and plating efficiency (58%) similar to that of *wild-type* TK6 cells. Like the DT40 mutants, human *SMARCAL1*$^{-/-}$ cells were moderately but also significantly sensitive to camptothecin (Figure 2A). Three *SMARCAL1*$^{-/-}$ clones and NHEJ-deficient *LIG4*$^{-/-/-}$ and *DNA-PKcs*$^{-/-}$, but not HR-deficient *RAD54*$^{-/-}$, were sensitive to ICRF193 (Figure 2B, Supplementary Figures S2C and S4B). Additionally, *LIG4*$^{-/-/-}$ and *SMARCAL1*$^{-/-}$/*LIG4*$^{-/-/-}$ cells showed the same sensitivity to ICRF193 (Figure 2D). Likewise, *DNA-PKcs*$^{-/-}$ and *SMARCAL1*$^{-/-}$/*DNA-PKcs*$^{-/-}$ cells showed the same sensitivity to ICRF193 (Supplementary Figure S4B). We thus conclude that Smarcal1 promotes the canonical NHEJ pathway in both DT40 and TK6 cell lines.

Human *SMARCAL1*$^{-/-}$ cells are defective for DSB repair in the G_1 phase

SMARCAL1$^{-/-}$ DT40 and TK6 cells were significantly radiosensitive (Figures 1C and 2C and Supplementary Figure S2C). Remarkably, *SMARCAL1*$^{-/-}$, *DNA-PKcs*$^{-/-}$ and *SMARCAL1*$^{-/-}$/*DNA-PKcs*$^{-/-}$ TK6 cells showed very similar radiosensitivity (Figure 2E and Supplementary Figure S4A). To further investigate the role of Smarcal1 in